Acta Crystallographica Section B
Structural Science
ISSN 0108-7681

An unexpected co-crystal with a variable degree of order: 1:1 *rac*-1,2-cyclohexanediol/triphenylphosphine oxide

Maxime A. Siegler, Yigang Fu, Greg H. Simpson, Daniel P. King, Sean Parkin and Carolyn Pratt Brock*

Department of Chemistry, University of Kentucky, Lexington, KY 40506-0055, USA

Correspondence e-mail: cpbrock@uky.edu

Received 12 June 2007
Accepted 30 October 2007

A 1:1 co-crystal of *rac-trans*-1,2-$C_6H_{10}(OH)_2$ and $(C_6H_5)_3PO$ has been found that is unusual because there are no strong interactions between the two kinds of molecules, which are segregated into layers. Furthermore, neither pure *rac*-1,2-cyclohexanediol (CHD) nor pure triphenylphosphine oxide (TPPO) has any obvious packing problem that would make the formation of inclusion complexes likely. The TPPO layers are very much like those found in two of the four known polymorphs of pure TPPO. The hydrogen-bonded ribbons of CHD are similar to those found in other *vic*-diol crystals. The co-crystals are triclinic (space group $P\overline{1}$), but the deviations from monoclinic symmetry (space group $C2/c$) are small. The magnitudes of those deviations depend on the solvent from which the crystal is grown; the deviations are largest for crystals grown from acetone, smallest for crystals grown from toluene, and intermediate for crystals grown from ethanol. The deviations arise from incomplete enantiomeric disorder of the *R*,*R* and *S*,*S* diols; this disorder is not required by symmetry in either space group, but occupancy factors are nearly 0.50 when the structure is refined as monoclinic. When the structure is refined as triclinic the deviations of the occupancy factors from 0.50 mirror the deviations from monoclinic symmetry because information about the partial *R*,*R*/*S*,*S* ordering is transmitted from one diol layer to the next through the very pseudosymmetric TPPO layer. Analyses suggest individual CHD layers are at least mostly ordered. The degree of order seems to be established at the time the crystal is grown and is unlikely to change with heating or cooling. Thermal data suggest the existence of the co-crystal is a consequence of kinetic rather than thermodynamic factors.

1. Introduction

In 1990 we discovered the very unusual layered compound[1] *rac-trans*-1,2-cyclohexanediol (hereafter, *rac*-1,2-CHD[2] or just CHD) and triphenylphosphine oxide (hereafter, TPPO), but were unable to publish its structure because important parts of the diffraction pattern were too weak to be measured well with the standard diffractometers then available. The compound (hereafter, CHDTPPO) is surprising because layers of hydrogen-bonded ribbons of *rac*-1,2-CHD molecules alternate with layers of TPPO molecules, even though there are no strong interactions between the two kinds of molecules to explain such a dramatic failure of fractional crystallization.

[1] The terms compound and co-crystal will be used interchangeably to describe this material. Another term would be molecular complex (see Herbstein, 2005).

[2] Nomenclature rules call for leaving out the *trans* identifier for these compounds when *rac*, *R*,*R* or *S*,*S* is used because all three imply a *trans* arrangement of the hydroxyl substituents. We have occasionally violated that rule in the interest of clarity.

CHDTPPO (see Fig. 1) can be viewed as a layered, molecular intercalate. The TPPO layer is very similar to that found in two of the four polymorphs of pure TPPO (Brock *et al.*, 1985; Spek, 1987; Lenstra, 2007); the *rac*-1,2-CHD hydrogen-bonded ribbons (or hydrogen-bonded ladders; see Fig. 2) are similar to those seen in other *vic*-diols (Brock, 2002), although not in pure *rac*-1,2-CHD (Lloyd *et al.*, 2007). There is no indication that the structure of either pure compound is unsatisfactory in a way that would make the formation of an inclusion complex likely. The densities of CHD and TPPO crystals are normal and all important donors and acceptors are satisfied.

Discovery of the compound was serendipitous. We had been looking at phase relationships in *cis*- and *trans*- (*i.e. rac*-, *R*,*R*- and *S*,*S*-) 1,2-CHD (see Lloyd *et al.*, 2007) and had found that the *rac*-1,2-CHD crystals grew as thin plates. Since in 1990 we had recently read the Etter & Baures (1988) paper titled 'Triphenylphosphine Oxide as a Crystallization Aid', we tried growing crystals from solutions equimolar in *rac*-1,2-CHD and TPPO. Crystallization from toluene produced attractive lath-like crystals containing both solutes.

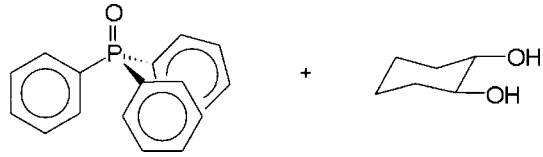

The structure of the CHDTPPO co-crystal could be solved, albeit with difficulty, but the refinement was problematic. While the structure was found to be triclinic with two pairs of molecules in the asymmetric unit ($Z' = 2$), it is almost monoclinic (space group $C2/c$) with $Z' = 1$. The average intensity of the reflections that would have monoclinic indices $h0\ell$, ℓ odd, was found to be extremely low. If the structure is treated as

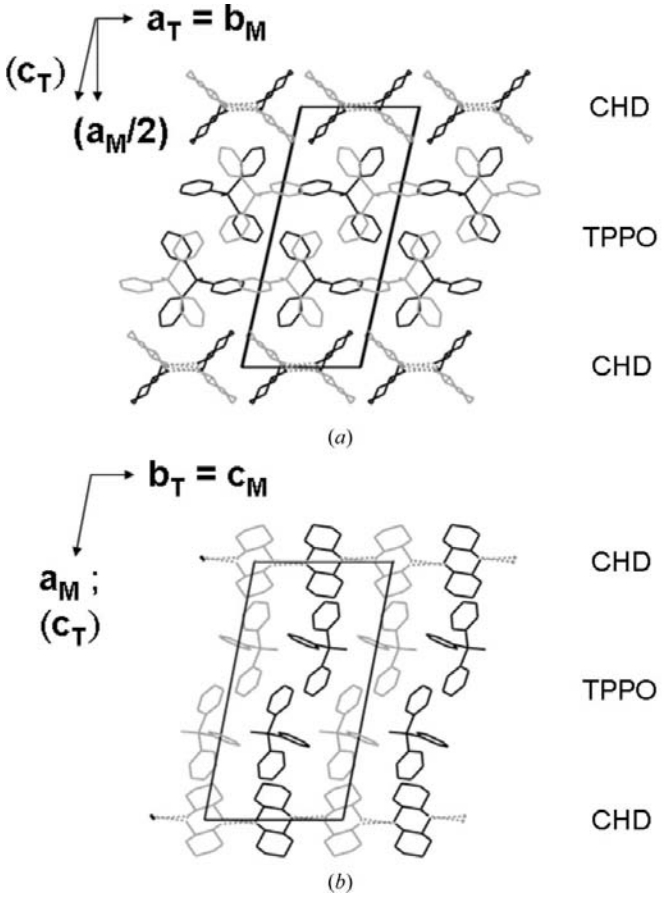

Figure 1
Two projections of an ordered triclinic structure of the 1:1 compound of *rac*-1,2-cyclohexanediol and triphenylphospine oxide. The two independent molecules of the two components are distinguished by the shade of gray. Both the triclinic and approximate monoclinic axes are shown; they are distinguished by subscripts. (*a*) Projection down $\mathbf{b}_T = \mathbf{c}_M$; (*b*) projection down $\mathbf{a}_T = \mathbf{b}_M$. Note that the $\mathbf{a}_T$ axis in (*a*) and the $\mathbf{b}_T$ axis in (*b*) are almost in the plane of the drawing because the angle γ_T is very close to 90° (see Table 1). In neither case, however, is the $\mathbf{c}_T$ axis (surrounded by parentheses) even approximately in the plane of the drawing. In (*a*) the $\mathbf{a}_M$ axis is not in the plane of the drawing either.

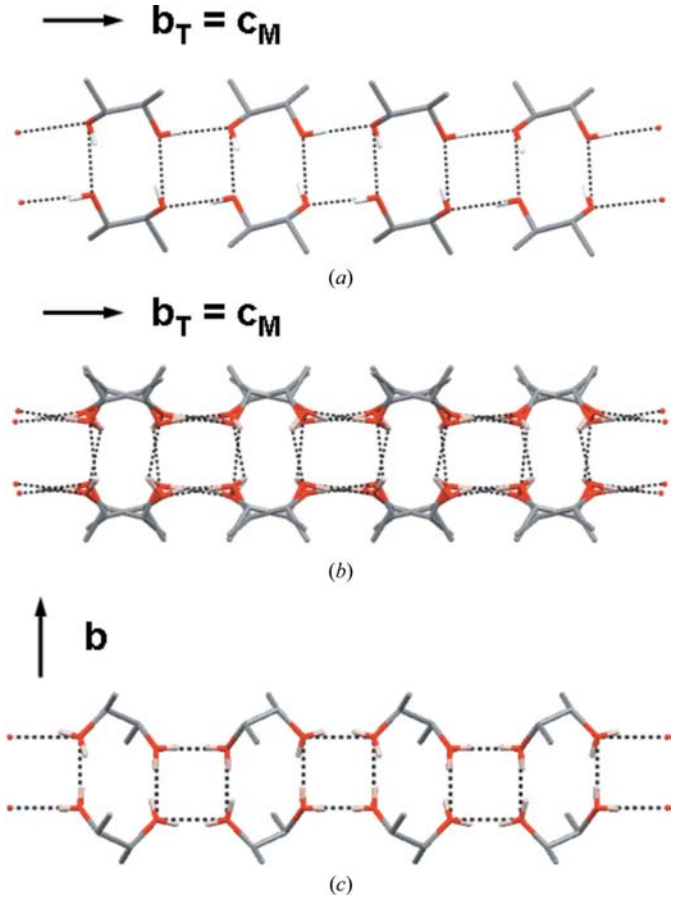

Figure 2
Perspective drawings of dimer ribbons formed by two *vic*-diols. The H atoms are shown for the hydroxyl groups only. All non-H atoms have been deleted except for those directly attached to the (HO)CC(OH) unit. (*a*) Dimer ribbon of *rac*-1,2-cyclohexanediol as it would appear in a completely ordered, triclinic crystal of the 1:1 compound of *rac*-1,2-CHD and triphenylphosphine oxide. (*b*) Dimer ribbon of *rac*-1,2-CHD as it would appear in a completely disordered, monoclinic crystal of the 1:1 compound of *rac*-1,2-CHD and triphenylphosphine oxide. (*c*) Dimer ribbon of *rac*-1,2-dicyclohexylethane-1,2-diol ($C2/c$, $Z' = 1$; Patrick & Brock, 2006). A comparison of the ribbons in (*a*) and (*c*) shows that the $R_4^4(8)$ hydrogen-bonded rings are much more square in the latter, but are also alternately displaced towards the two sides of the ribbon, *i.e.* along **b**.

Table 1
Experimental details.

Details of all the data collected can be found in the CIF file which has been deposited.

	From acetone	From ethanol	From toluene
Crystal data			
Chemical formula	$C_6H_{12}O_2{\cdot}C_{18}H_{15}OP$	$C_6H_{12}O_2{\cdot}C_{18}H_{15}OP$	$C_6H_{12}O_2{\cdot}C_{18}H_{15}OP$
M_r	394.43	394.43	394.43
Cell setting, space group	Triclinic, $P\overline{1}$	Triclinic, $P\overline{1}$	Triclinic, $P\overline{1}$
Temperature (K)	90.0 (2)	90.0 (2)	90.0 (2)
a, b, c (Å)	9.276 (1), 10.913 (1), 21.256 (2)	9.273 (1), 10.919 (1), 21.262 (2)	9.271 (1), 10.923 (1), 21.306 (2)
α, β, γ (°)	100.58 (1), 102.52 (1), 90.51 (1)	100.66 (1), 102.56 (1), 90.23 (1)	100.77 (1), 102.53 (1), 90.02 (1)
V (Å^3)	2062.2 (4)	2062.8 (4)	2067.2 (4)
Z	4	4	4
D_x (Mg m^{-3})	1.270	1.270	1.267
Radiation type	Mo $K\alpha$	Mo $K\alpha$	Cu $K\alpha$
μ (mm^{-1})	0.16	0.16	1.35
Crystal form, color	Lath, colorless	Lath, colorless	Lath, colorless
Crystal size (mm)	0.25 × 0.21 × 0.13	0.25 × 0.20 × 0.12	0.20 × 0.12 × 0.04
Data collection			
Diffractometer	Nonius KappaCCD	Nonius KappaCCD	Bruker–Nonius X8 Proteum
Data collection method	1.0° ω scans at fixed χ = 55°	1.0° ω scans at fixed χ = 55°	ω and φ scans
Absorption correction	Multi-scan (based on symmetry-related measurements)	Multi-scan (based on symmetry-related measurements)	Multi-scan (based on symmetry-related measurements)
T_{min}	0.96	0.96	0.77
T_{max}	0.98	0.98	0.95
No. of measured, independent and observed reflections	14 392, 7244, 4848	14 485, 7244, 4413	28 054, 7346, 6312
Criterion for observed reflections	$I > 2\sigma(I)$	$I > 2\sigma(I)$	$I > 2\sigma(I)$
R_{int}	0.052	0.065	0.055
θ_{max} (°)	25.0	25.0	68.2
Refinement			
Refinement on	F^2	F^2	F^2
$R[F^2 > 2\sigma(F^2)]$, $wR(F^2)$, S	0.049, 0.122, 1.06	0.049, 0.116, 1.00	0.039, 0.098, 1.04
No. of reflections	7244	7244	7346
No. of parameters	564	564	564
H-atom treatment	Constrained to parent site	Constrained to parent site	Constrained to parent site
Weighting scheme	$w = 1/[\sigma^2(F_o^2) + (0.0595P)^2]$, where $P = (F_o^2 + 2F_c^2)/3$	$w = 1/[\sigma^2(F_o^2) + (0.0514P)^2]$, where $P = (F_o^2 + 2F_c^2)/3$	$w = 1/[\sigma^2(F_o^2) + (0.0363P)^2 + 0.8227P]$, where $P = (F_o^2 + 2F_c^2)/3$
$(\Delta/\sigma)_{max}$	0.001	0.001	0.002
$\Delta\rho_{max}$, $\Delta\rho_{min}$ (e Å^{-3})	0.35, −0.29	0.30, −0.28	0.29, −0.42

Computer programs used: *COLLECT* (Nonius, 1999), *APEX2* (Bruker–Nonius, 2004), *SCALEPACK* (Otwinowski & Minor, 1997), *Saintplus in APEX2* (Bruker–Nonius, 2004), *DENZO-SMN* (Otwinowski & Minor, 1997), *MULTAN* (Main *et al.*, 1977), *DIRDIF* (Beurskens *et al.*, 1983), *SHELXL97* (Sheldrick, 1997), *MERCURY* (Macrae *et al.*, 2006), and local procedures.

monoclinic there is nearly complete disorder of *R*,*R*- and *S*,*S*-1,2-CHD molecules. If the structure is treated as triclinic it is more ordered but not completely ordered.

We returned to this project only recently after new hardware and software had become available. A Nonius KappaCCD diffractometer measured the intensities of the weak reflections much more reliably than the serial diffractometer it replaced, and the new diffractometer and its software allowed the display of both the Bragg and non-Bragg scattering in reciprocal-lattice slices. The program *PLATON* (Spek, 2003) found evidence of pseudomerohedral twinning, which we had missed, and the program *MERCURY* (Macrae *et al.*, 2006) greatly facilitated the comparison of the structures. Finally, the recognition of the importance of C—H···O= interactions (Desiraju, 1996; Jeffrey, 1997; Desiraju & Steiner, 1999) made the structures of the pure TPPO polymorphs easier to understand.

While looking at this problem again we were surprised to discover that the magnitudes of the deviations from the monoclinic symmetry seem to depend on the identity of the solvent from which the crystals are grown. We were also surprised to discover that the deviations from monoclinic symmetry require that there be correlation between *rac*-1,2-CHD layers separated by a TPPO layer even though the deviations from monoclinic symmetry within the TPPO layers are very small.

This structure then raises a number of questions. First, why does the compound form? Why does fractional crystallization fail? Second, how is information about ordering of the *rac*-1,2-CHD layers transmitted through TPPO layers? Finally, why

does the degree of order vary with the solvent from which the crystals are grown?

2. Experimental

2.1. Crystal growth and morphology

Colorless crystals were grown by the slow evaporation at room temperature of acetone, ethanol and toluene solutions equimolar in *rac*-1,2-CHD and TPPO. Crystallization from acetonitrile gave no macroscopic crystals. Crystallizations were carried out in small vials and Petri dishes covered with parafilm in which several holes had been made with a fine sewing needle. Crystals grew from acetone in 1–2 d and from ethanol in 3–5 d, but crystallization from toluene took more than a week, even though solubility is lowest in toluene. The crystals grown from toluene had the best looking faces.

Most evaporation dishes and vials held numerous crystals having obvious faces, although a few evaporations yielded only fine-grained material. Crystals are longest in the direction of the hydrogen-bonded ribbons ($\mathbf{b}_T = \mathbf{c}_M$, where the subscripts distinguish between the triclinic and monoclinic axial systems). Two types of crystal habit were seen (see Fig. 3). Some crystals grew as thin (sometimes very thin) tablets with pointed ends; others grew as longer and usually thicker parallelepipeds with ends capped by a single face. Both crystal types have the same crystal structure but many of the larger tablets had small re-entrant angles between faces intersecting in a line parallel to $\mathbf{b}_T$ (*i.e.* the direction in which the crystals are longest) and those crystals were therefore identified as twinned. We saw no indication of the presence of any phase of pure TPPO or *rac*-1,2-CHD in the many crystallization vials and dishes we examined that contained macroscopic crystals.

The most prominent faces of the crystals seemed at first to belong to the forms $\{1\,0\,0\}_T$ and $\{0\,0\,1\}_T$, with the former sometimes considerably larger than the latter. It is probable, however, that what might be the $\{1\,0\,0\}_T$ form is, at least most of the time, actually the $\{2\,0\,\bar{1}\}_T$ form, which would be the $\{0\,1\,0\}_M$ form if the symmetry were monoclinic. The angle between $(1\,0\,0)_T$ and $(2\,0\,\bar{1})_T$ is only 12.7°, so distinguishing between the two possible forms is not so easy. The twinning would lead to obvious re-entrant angles (*ca* 25°) if the large faces belonged to the form $\{1\,0\,0\}_T$, but to much smaller angles (< 1°) if the faces belonged to the form $\{2\,0\,\bar{1}\}_T$. Sometimes, but not always, we could see very small re-entrant angles involving the larger faces.

Identification of the end faces was much more difficult. The pictures shown in Fig. 3, which was drawn with the program *SHAPE* (Shape Software, 2003), are labeled with the indices of the forms that we found gave the best facsimiles of the crystals we observed.

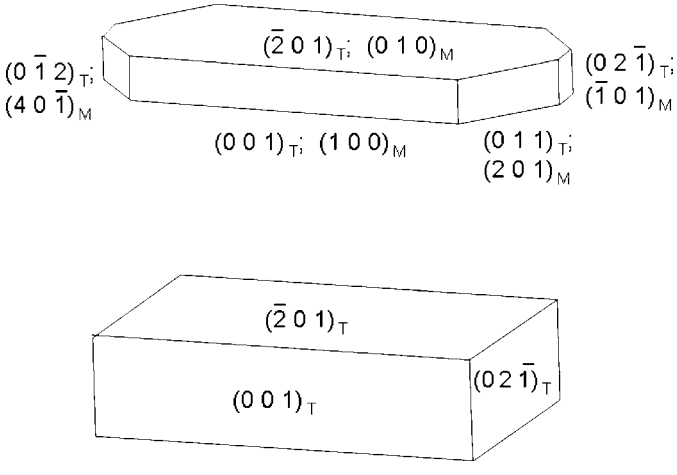

Figure 3
Habits of typical crystals of the 1:1 compound of *rac*-1,2-CHD with triphenylphosphine oxide. The largest face has been labeled as $(\bar{2}\,0\,1)_T$ rather than as $(1\,0\,0)_T$, because the latter choice leads to obvious re-entrant angles when the twinning operation (a twofold axis parallel to $\mathbf{a}_T$ or a mirror perpendicular to that axis) is introduced.

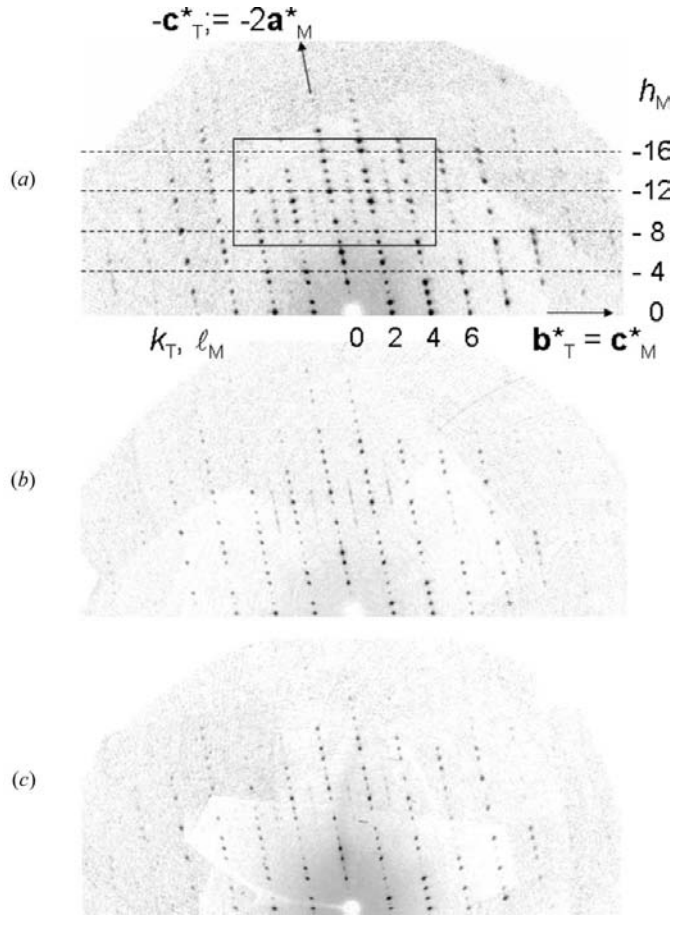

Figure 4
Parts of reconstructed $(h0\ell)_M = (0k\ell)_T$ planes of the reciprocal lattices of crystals grown from (*a*) acetone, (*b*) ethanol and (*c*) toluene, and measured at 90 K on the Nonius KappaCCD diffractometer. The reciprocal axes shown for (*a*) are the same for (*b*) and (*c*). The index values shown to the right of the pattern are h_T; because the monoclinic cell is centered all reflections have $h_M = 2h_T$. The box outlines the area that is enlarged in the following figure.

Table 2
Measures of the deviations of the diffraction patterns from monoclinic symmetry.

For the sake of consistency the results given for the crystal grown from toluene are from the data collected with Mo $K\alpha$ radiation rather than for the data collected with Cu $K\alpha$ radiation. The values for the crystal grown from toluene therefore differ from those given in Table 1.

Solvent from which crystals were grown; T for data collection	From acetone	From ethanol	From toluene
α, γ (°) for the monoclinic setting	90.51 (1), 89.92 (1)	90.23 (1), 89.96 (1)	90.12 (1), 89.98 (1)
Number of h0ℓ, $\ell = 2n + 1$ reflections (monoclinic indexing) with $I > n\sigma(I)$, n = 2, 5, 10, 20, 50	245, 185, 146 109, 35 (of 488)	212, 161, 121 89, 26 (of 489)	208, 153, 114 78, 20 (of 487)
R_{int} for averaging in $P\bar{1}$ and in $C2/c$	0.052	0.064	0.079
(the latter without its $h0\ell$, $\ell = 2n + 1$ reflections)	0.179	0.119	0.098
$\langle\sigma(I)/I\rangle$, No. with $I > 2\sigma(I)$ in $P\bar{1}$, $C2/c$	0.074; 4848 (of 7244)	0.093; 4413 (of 7244)	0.115; 4339 (of 7254)
	0.104; 2713 (of 3630)	0.077; 2527 (of 3631)	0.073; 2495 (of 3634)
R_1, wR_2 for $P\bar{1}$ and $C2/c$ refinements	0.049, 0.122	0.049, 0.116	0.054, 0.111
	0.074, 0.121	0.053, 0.107	0.057, 0.112
$P\bar{1}$ larger twin fraction in $P\bar{1}$ refinement	0.873 (2)	0.787 (3)	0.570 (3)
Larger occupancy factors in $P\bar{1}$ refinement	0.800 (5)	0.700 (5)	0.651 (6)
	0.882 (6)	0.759 (6)	0.795 (9)

2.2. Structure determinations

Data were collected at 90 and 294 K for crystals that looked single (but were not) and that had been grown from acetone, ethanol and toluene (see Table 1 and the supplementary material[3]). Different crystals were used for the low- and room-temperature data collections. The estimated errors shown for the unit-cell constants (see Table 1) were obtained by multiplying the experimental estimated uncertainties by a factor of 3 for the cell lengths and by a factor of 20 for the cell angles. These factors were introduced in order to account for differences between cell constants determined for crystals grown under the same conditions.

The diffraction patterns can be indexed in a C-centered monoclinic cell with $Z = 8$ and $Z' = 1$, but the cell angles α and γ deviate significantly from 90° and the agreement factors for averaging in Laue group $2/m$ are substantially larger than expected (see Table 2). Most of the reflections $h0\ell$, $\ell = 2n + 1$ (monoclinic indices), are very weak, but in most crystals a number of those reflections are clearly present although occasionally diffuse (see Figs. 4–6).

We concluded in 1990 and again recently that the best unit cell, at least for most crystals, is triclinic (space group $P\bar{1}$) with $Z = 4$ and $Z' = 2$. The transformation between the monoclinic unit cell and the triclinic cell is given by

$$\mathbf{a}_T = (0\,1\,0/0\,0\,1/\tfrac{1}{2}\;-\tfrac{1}{2}\;0)\mathbf{a}_M$$

and

$$\mathbf{a}_M = (1\,0\,2/1\,0\,0/0\,1\,0)\mathbf{a}_T.$$

The monoclinic cell dimensions are 41.51 (1), 9.276 (2), 10.916 (2) Å and 90, 100.96 (2), 90° at 90 K (the uncertainties reflect the differences between crystals grown from different

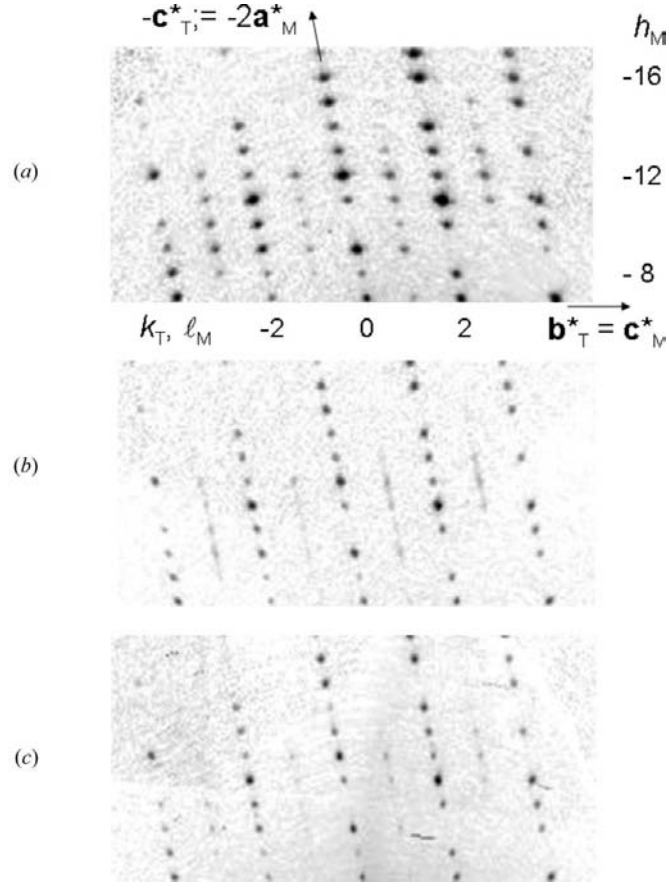

Figure 5
Enlargements of selected areas of the $h0\ell$ planes shown in Fig. 4. The $(h0\ell)_M$, $\ell_M = 2n + 1$ reflections [or $(0k\ell)_T$, $k_T = 2n + 1$ reflections] are systematically weak. They are always weaker and more diffuse for crystals grown from ethanol and toluene [see parts (*b*) and (*c*)] than for crystals grown from acetone [see part (*a*)].

[3] Supplementary data for this paper are available from the IUCr electronic archives (Reference: DE5032). Services for accessing these data are described at the back of the journal.

solvents) when α and γ are constrained to be 90°. The dimensions of the triclinic cells are shown in Table 1. Some unconstrained values of α and γ are given in Table 2.

Note that the transformation shown in the previous paragraph does not always give the conventional reduced unit cell (Niggli, 1928) because the cell dimensions are just at the point where very small changes in the dimensions lead to a discontinuous change in the reduced cell (see Andrews *et al.*, 1980, and references therein). The 'other' triclinic cell has the same cell lengths, but the cell angles are the supplements (*i.e.* $\alpha' = 180 - \alpha$) of the values given in Table 1.

Refinements using data collected with a Nonius KappaCCD diffractometer were straightforward once the twin model suggested by the program *PLATON* (Spek, 2003) [twin matrix for the triclinic unit cell is (1 0 0 / 0 −1 0 / −1 0 −1)] had been included. This twin operation corresponds to a twofold rotation around the axis $\mathbf{b}_M$ of the pseudomonoclinic cell or the $\mathbf{a}_T$ axis of the triclinic cell. The twin operation could, however, just as well have been chosen to be a mirror plane perpendicular to $\mathbf{b}_M = \mathbf{a}_T$.

The structure can also be refined well in the approximate monoclinic cell, although the results are better for some crystals than for others (see Table 2). The atomic ellipsoids determined using space group *C*2/*c* are unremarkable, even for the crystals that deviate most from monoclinic symmetry (see Fig. 7, which also shows the atom-numbering scheme). These ellipsoids are very similar (except as described below) to those determined when the structure was treated as triclinic. In the monoclinic refinements the occupancy factors for the disordered *R*,*R* and *S*,*S* *rac*-1,2-CHD molecules are very nearly 0.5 [deviations from 0.500 are in the range 0.001 (7)–0.039 (6)].

At first we thought that the hydrogen-bonded *rac*-1,2-CHD ribbons in the triclinic cell were ordered, but then noticed that some of the atomic ellipsoids for *rac*-1,2-CHD atoms were elongated perpendicular to the ring plane in a way that suggested disorder. The final structural model included superimposed *R*,*R* and *S*,*S*-1,2-CHD molecules; distances between nearly overlapping atoms are 0.2–0.7 Å. Pairs of closely spaced atoms of superimposed *R*,*R*- and *S*,*S*-1,2-CHD molecules were required to have the same displacement parameters (instruction EADP); the displacement parameters were also subject to a rigid-bond restraint (instruction DELU 0.005). Corresponding bond lengths (1,2 distances) and 1,3 distances in superimposed molecules were restrained to be equal (instruction SAME 0.006). Refined occupancy factors are shown in Table 2, as are the refined twin fractions.

The atomic displacement ellipsoids for crystals grown from acetone and ethanol were unremarkable, but the atomic displacement ellipsoids for crystals grown from toluene were found to be quite eccentric, particularly at 90 K (see Fig. 8).

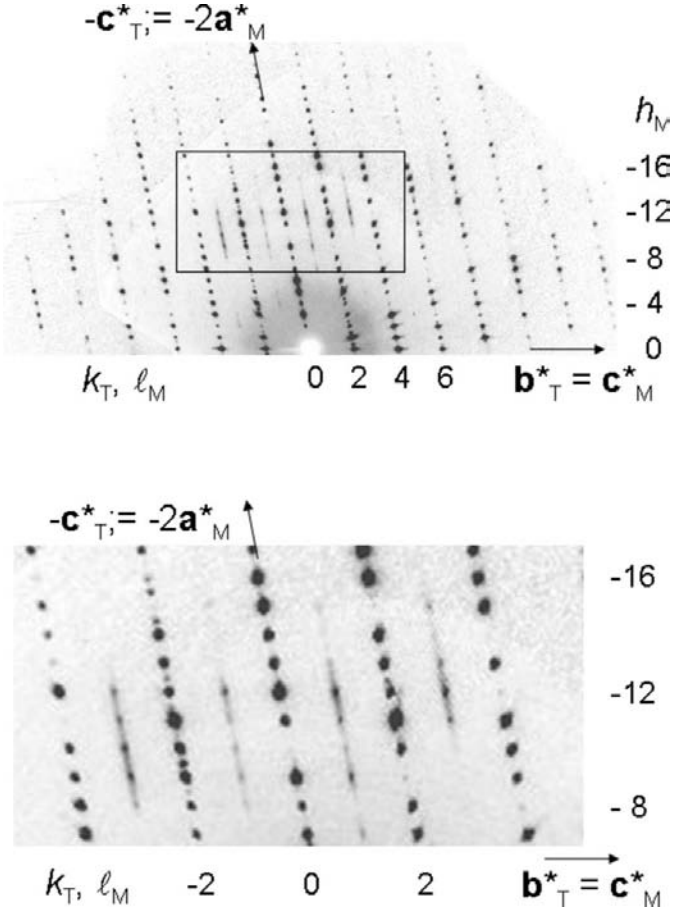

Figure 6
Patterns analogous to those shown in Figs. 4 and 5 for one crystal grown from toluene. There is very significalnt streaking and some extra spots are present. No refinement of the data from this crystal is reported.

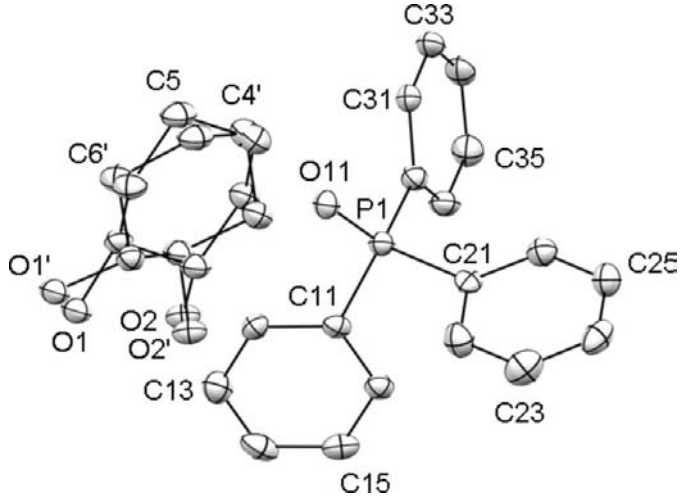

Figure 7
Ellipsoid plot for the refinement in the monoclinic pseudocell of the data collected at 90 K from a 1:1 co-crystal of *rac*-1,2-CHD and TPPO grown from acetone. While some of the ellipsoids are just a little larger than might be expected for a crystal studied at 90 K, none is especially large or eccentric. Deviations from monoclinic symmetry increase as the temperature is lowered and are largest for crystals grown from acetone, so the displacement ellipsoids (50% probability level) for the other five *C*2/*c* refinements are even less affected by the inappropriate averaging than those shown here. H atoms have been omitted for the sake of clarity. All atom labels can be worked out from those shown; atoms in the two independent sets of molecules (not shown in this drawing) are distinguished by an *A* or *B* at the end of the label. Molecule *A* is closer to $y = \frac{1}{4}$ while molecule *B* is closer to $y = \frac{3}{4}$.

For the crystal grown from toluene and studied at 90 K the displacement parameters for superimposed atoms C4*A* and C4*A*′ of the *rac*-1,2-CHD molecule A were even non-positive definite. Ellipsoids for some pairs of atoms related by the pseudosymmetry are elongated in roughly orthogonal directions, as they would be if correlation were important; absolute values of correlation coefficients were as large as 0.84. There was no easy way to resolve this problem without applying strong restraints (instruction ISOR) or constraints (strictly isotropic refinement) because the axis $\mathbf{c}_T$ makes an angle of *ca* 103° with the axis $\mathbf{a}_T$, which is perpendicular to the pseudo-glide plane.[4] In any event we eventually concluded that the reflection intensities for the crystal grown from toluene had not been measured well enough at 90 K with Mo *Kα* radiation to support refinement in the pseudosymmetric triclinic cell. The refinement of the data measured at 294 K was less of a problem because of the larger average volume of the ellipsoids. Refinements at 90 K of crystals grown from acetone and ethanol were much more satisfactory because the deviations from monoclinic symmetry were larger.

We later collected data at 90 K for a crystal grown from toluene with a more powerful diffractometer [a Bruker–Nonius X8 Proteum diffractometer that used Cu *Kα* radiation from a rotating-anode source, that had Bruker Helios graded multilayer focusing optics, and that was equipped with a CRYOCOOL-LN2 low-temperature system (CRYO Industries of America, Manchester, NH)]. It is our experience that there is a greater than 10^3-fold increase in recordable diffracted X-rays in going from our standard KappaCCD instrument with its sealed-tube Mo *Kα* source to this instrument. The data measured with Cu *Kα* radiation gave a satisfactory refinement of the structure at 90 K of a crystal grown from toluene (see Table 1). Minor abnormalities can still be spotted in the atomic displacement ellipsoids, but there is no feature as troublesome as in Fig. 8 and all displacement functions are positive definite.

For all refinements the H atoms attached to C atoms were placed in calculated positions (AFIX 13, 23 or 43 as appropriate) with $U_{iso} = 1.2*U_{eq,C}$. Many of the hydroxyl H atoms for the major *rac*-1,2-CHD sites could be located in difference maps. All were included in the structural model with fixed geometry, a variable C—C—O—H torsion angle (AFIX 147) and $U_{iso} = 1.5*U_{eq,O}$ (see Fig. 2).

Restraints and constraints for the disordered C and O atoms were the same in the monoclinic refinement as in the triclinic refinement. The disordered hydroxyl H atoms that form hydrogen bonds between *rac*-1,2-CHD molecules related by the twofold rotations (*i.e.* the hydrogen bonds of the rails of the hydrogen-bonded ladder) were easy enough to locate, but the hydroxyl H atoms that form hydrogen bonds between molecules related by inversion centers (*i.e.* the hydrogen bonds of the ladder rungs) were not. If the O—H distance and C—O—H angle were required to have standard values then the O—H···O angle was too small and some of the H atoms were significantly displaced from the ring of four O atoms. We tried forcing *SHELXL*97 to locate these atoms by specifying AFIX 143 (fixed C—O—H geometry) and the coordinates of the expected acceptor O atom, but the program could not find acceptable H-atom positions [see part (*b*) of Fig. 2]. The positions of some of the hydroxyl H atoms that have been deposited are therefore approximate at best. We believe the difficulties locating these H atoms suggest that individual hydrogen-bonded chains are ordered (see §3.3.1).

We also encountered problems when trying to locate the hydroxyl H atoms of the lower-occupancy sites of the triclinic refinement. Refinements of data measured at 90 K (but not the data measured at 294 K) led to some hydroxyl H-atom positions for the minor sites that were not near any good hydrogen-bond acceptor. We eventually decided to leave the offending H atoms in these positions because despite much effort we were unable to find any structural model that was more satisfactory.

Table 1 shows the results for crystals grown from the three solvents, studied at 90 K and refined as triclinic. Information about the refinements of the three sets of data collected at room temperature are included with the supplementary material, which also includes results for all the refinements in which the structures were treated as monoclinic.

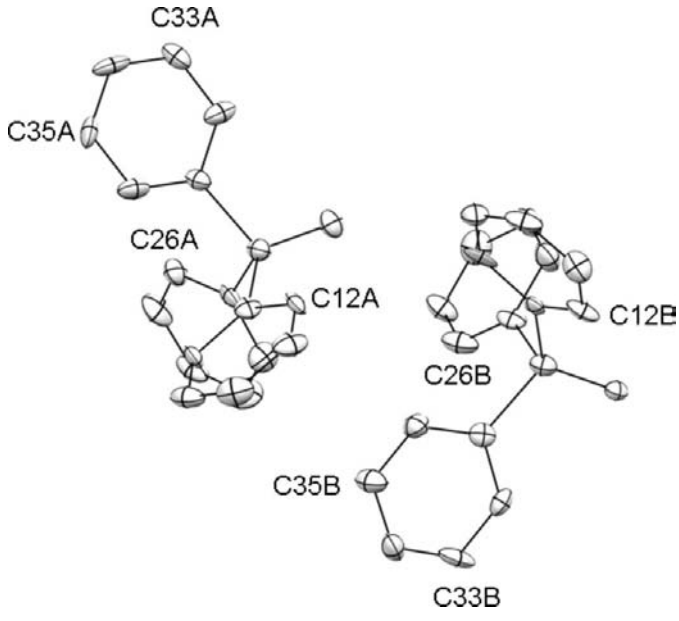

Figure 8
Perspective drawing showing ellipsoids determined at 90 K for the two independent TPPO molecules in a 1:1 co-crystal of *rac*-1,2-CHD and TPPO grown from toluene. The two molecules are related by the pseudo-glide plane of the approximate *C*2/*c* cell; the $\mathbf{b}_T = \mathbf{c}_M$ axis is approximately horizontal. The correlation resulting from the pseudosymmetry is responsible for the displacement ellipsoids of some pairs of corresponding atoms being elongated in roughly orthogonal directions. The ellipsoids determined at 294 K are both larger and less eccentric.

[4] In order to constrain the ellipsoids of pseudosymmetrically related atoms to be equal we would have had to refine the structure in $C\bar{1}$ (same axes as for *C*2/*c*) rather than in $P\bar{1}$, and would have had to use free variables for the six U^{ij} values of each constrained atom so that U^{12} and U^{23} for the related atoms could have opposite signs.

Table 3
Packing coefficients and intermolecular $P{=}O\cdots H{-}C$ contacts (Å) with $O\cdots H$ distances less than 275 Å.

	Space group; Z'	Packing coefficient near 294 K	$O\cdots H$ contacts near 90 K	$O\cdots H$ contacts near 294 K
TPPO, orthorhombic	*Pbca*; 1	0.650	2.39, 2.52, 2.59	2.34, 2.50, 2.62
TPPO, 1st monoclinic	$P2_1/c$; 1	0.654	2.50, 2.63, 2.63	2.60, 2.72, 2.74
TPPO, 2nd monoclinic	$P2_1/c$; 1	0.640	–	2.46, 2.58, 2.65
TPPO, 3rd monoclinic	$P2_1/n$; 1	0.653	–	2.38, 2.66
CHDTPPO	$P\bar{1}$; 2	0.661	2.46, 2.57, 2.58 2.42, 2.57, 2.58	2.53, 2.65, 2.69 2.49, 2.66, 2.68

References, CHDTPPO at 90 K, this work; crystal grown from acetone; orthoTPPO at 100 K, Brock *et al.* (1985); orthoTPPO at room temperature, Thomas & Hamor (1993); first monoTPPO at 100 K, Brock *et al.* (1985); first monoTPPO at room temperature, Falvello *et al.* (2002); second monoTPPO at room temperature, Spek (1987); third monoTPPO at room temperature, Lenstra (2007). The low-temperature structures of the seond and third monoclinic TPPO polymorphs have never been reported. The packing coefficients for the room-temperature structures of CHDTPPO and the first monoclinic polymorph were calculated using *PLATON* (Spek, 2003). The packing coefficients for these two structures are comparable because both have the $C_{Ar}{-}H$ distances (0.93 Å). Packing coefficients for the other TPPO polymorphs were then determined from that of the first monoclinic polymorph by multiplication by the ratios of the molar volumes.

2.3. Thermal measurements

Differential scanning calorimetry (hereafter DSC) measurements were performed in 1990 on a Perkin-Elmer 7 Series Thermal Analysis System and again in 2006 on a TA Instruments 2920 Modulated DSC apparatus. In 1990 the heating rate was 10 K min^{-1}; in 2006 it was usually 2 K min^{-1}, but some scans were also made at 1 and 5 K min^{-1} to be sure the results were independent of heating rate. At least two samples of each of the following were studied: *rac*-1,2-CHD, TPPO, a 1:1 (mole basis) physical mixture of *rac*-1,2-CHD and TPPO and material precipitated from solutions equimolar in *rac*-1,2-CHD and TPPO. All pure compounds were taken directly from the bottles of purchased chemicals.

The melting points given by Aldrich (374–377 K for *rac*-1,2-CHD; 429–431 K for TPPO) were confirmed. There are four known polymorphs for TPPO (Brock *et al.*, 1985; Spek, 1987; Lenstra, 2007; see Table 3), but there is no evidence in the literature that their melting points or $\Delta_{fus}H^\circ$ values differ measurably. We saw no evidence of any solid-solid phase transition.

We found an endotherm at 338–344 K with $\Delta_{trans}H^\circ$ of 2–3 kJ mol^{-1} for *rac*-1,2-CHD in 2006, but not in 1990. Presumably this endotherm corresponds to the transition from the *Pbca* phase to the *C*2/*c* phase (Lloyd *et al.*, 2007) and was missed when the heating rate was 10 K min^{-1}. The values of $\Delta_{fus}H^\circ$ for *rac*-1,2-CHD were found to be 20.5 kJ mol^{-1} in 1990 when the solid–solid transition was not observed and 17 kJ mol^{-1} in 2006 when it was. The values of $\Delta_{fus}H^\circ$ for TPPO were somewhat variable: 16 kJ mol^{-1} in 1990 and 24 kJ mol^{-1} in 2006. It could be that the polymorphs might have somewhat different $\Delta_{fus}H^\circ$ values even if their melting points are similar and that the phase ratios in the samples we studied were not always the same.

Material precipitated from solutions equimolar in *rac*-1,2-CHD and TPPO and physical mixtures of *rac*-1,2-CHD and TPPO both melted in the range 351–357 K and had $\Delta_{fus}H^\circ$ for the 1:1 compound in the range 33–37 kJ mol^{-1}.

2.4. CSD searches

A search was made of the November 2006 version (5.28) and January 2007 update of the Cambridge Structural Database (Allen, 2002; hereafter, the CSD) for structures containing $Ph_3P{=}O$ and having no metal present, coordinates archived and $R < 0.10$. There were 90 hits, of which 11 were structures of pure TPPO and another was a mixed crystal of $Ph_3P{=}O$ and $Ph_3P{=}S$. Of the remaining 78, five were duplicates and all but seven of the others had bonds to obvious H donors in other molecules or ions (water, organic acids, phenols, amines, a protonated TPPO *etc.*). Six of the remaining seven had more exotic interactions that could still be easily classified as hydrogen bonds or Lewis acid–base interactions. In the last compound (refcode NUCHIC) the $P{=}O$ bond of TPPO makes a perpendicular approach to an $N_{Ar}C(=O)N_{Ar}$ group ($O\cdots C$. 2.93 Å). In all compounds found (with the possible exception of NUCHIC) there was an obvious strong interaction between the two components. The CHDTPPO compound reported in this paper is very unusual in that it is a 1:1 compound including TPPO in which there are no strong interactions between the two components.

Most of the structures in the CSD in which the hydrogen-bond donor was a hydroxyl group were phenols, which are more acidic than alcohols, but four structures were found in which TPPO accepts a proton from a hydroxyl group attached to an aliphatic C atom (refcodes FAXRAX, KANDEI, LUMYIB and LUMYOH). The first two of these structures was known in 1990. We also happened to come across a structure (refcode CALGIF) of a metal complex that also contains an uncoordinated alcohol that is a hydrogen-bond donor to an uncoordinated TPPO molecule. We conclude that *rac*-1,2-CHD should be a strong enough acid to form a hydrogen bond to TPPO.

We also searched the CSD to find structures of *vic*-diols $C_nH_m(OH)_2$ that had been published since we reviewed their hydrogen-bond patterns (Brock, 2002), but found no structure that caused us to revise the conclusions of that paper.

Table 4
Comparison of cell constants for 1:1 *rac*-1,2-cyclohexanediol/triphenylphosphine oxide (CHDTPPO; triclinic axes) and the orthorhombic and second monoclinic polymorphs of triphenylphosphine oxide (TPPO).

	Near 90 K	Near 294 K
CHDTPPO/TPPO		
$b_{CHDTPPO,T}/c_{orthoTPPO}$	0.983	0.976
$b_{CHDTPPO,T}/c_{monoTPPO}$	–	0.974
$a_{CHDTPPO,T}/b_{orthoTPPO}$	1.022	1.022
$a_{CHDTPPO,T}/b_{monoTPPO}$	–	1.034
$\gamma_{CHDTPPO,T} - 90$ (°)	0.51	0.50
$TPPO_{ortho}/TPPO_{mono}$		
$c_{orthoTPPO}/c_{monoTPPO}$	–	1.012
$b_{orthoTPPO}/b_{monoTPPO}$	–	0.997

References: CHDTPPO at 90 K, this work; crystal grown from acetone; orthoTPPO at 100 K, Brock *et al.* (1985); orthoTPPO at room temperature, Thomas & Hamor (1993); monoTPPO at room temperature, Spek (1987). The low-temperature structure of the second monoclinic TPPO polymorph has never been reported.

3. Results

3.1. Disorder and twinning

The disorder and twinning (see Table 2) are greater in CHDTPPO crystals grown from ethanol than in crystals grown from acetone, and greatest for crystals grown from toluene. The lengths a_T and b_T do not change appreciably (see Table 1) between crystals grown from these different solvents, but the changes in the length c_T, which measures the interlayer spacing, are larger: 0.016 Å at 90 K and 0.013 Å at 294 K with an estimated uncertainty of no more than 0.003 Å. The length c_T is smallest for the crystals grown from acetone and largest for crystals grown from toluene, so an increase in disorder is associated with a small increase in the interlayer spacing.

Separate Wilson plots (Xia *et al.*, 2001, 2002) for the $(h0\ell)_M$, ℓ odd and even reflections, are shown in Fig. 9:

(i) for the data measured at 90 K for a crystal grown from acetone and measured with Mo $K\alpha$ radiation from a sealed-tube source, and

(ii) for a crystal grown from toluene and measured with Cu $K\alpha$ radiation from a rotating-anode source.

The $(h0\ell)_M$, ℓ odd reflections, are systematically weaker (by a factor of three) relative to the $(h0\ell)_M$, ℓ even reflections for the crystal grown from toluene than for the crystal grown from acetone even though the absolute intensities of the observed $(h0\ell)_M$, ℓ odd reflections were much greater for the toluene crystal than for the acetone crystal. These plots are further evidence for the greater deviations from monoclinic symmetry for crystals grown from acetone relative to crystals grown from toluene.

The refinements carried out for data collected at room temperature on different crystals gave very similar results for twin fractions as did the refinements of the data collected at 90 K, even though different crystals were used at the two temperatures. For the crystals grown from acetone, ethanol and toluene and studied at 294 K the corresponding twin fractions are 0.951 (2), 0.746 (2) and 0.584 (3). The twin fraction for the crystal grown from toluene and studied at 90 K using Cu $K\alpha$ radiation was 0.505 (2). The differences between these values and those shown in Table 2 are an indication of how the twin fraction varies from crystal to crystal. Full details of the refinements of the data collected at 294 K are given in the CIF.

3.2. TPPO layers

The two TPPO molecules of the asymmetric unit of CHDTPPO are related by a pseudo b_T glide perpendicular to $\mathbf{a}_T$. If orientations only are considered the two TPPO molecules can be superimposed (*r.m.s.* deviations 0.02–0.04 Å for the six structures) using the routine AutoMolFit of the program *PLATON* (Spek, 2003) by a rotation that differs from 180° by no more than 1° around an axis that is nearly parallel to $\mathbf{a}_T$.

The TPPO layers in CHDTPPO strongly resemble (see Fig. 10) those in the *Pbca* (*i.e.* the orthorhombic) polymorph of pure TPPO (Brock *et al.*, 1985); the TPPO layers in the CHDTPPO compound are nearly superimposable with the $\frac{1}{4} \leq x \leq \frac{3}{4}$ layers of the *Pbca* polymorph. There are also very strong similarities between the TPPO layer of the CHDTPPO structure and the $-\frac{1}{2} \leq x \leq \frac{1}{2}$ layers of the second monoclinic polymorph (Spek, 1987) of pure TPPO.

Note that orthorhombic TPPO can be viewed as a kind of superstructure of the second monoclinic polymorph of TPPO, although it seems very unlikely that a transformation between the two could occur without significant crystal damage. The cell relationships for the coordinates archived in the CSD are $\mathbf{b}_{ortho}$ parallel $-\mathbf{b}_{mono}$ and $\mathbf{c}_{ortho}$ parallel $-\mathbf{c}_{mono}$; length ratios are given near the end of Table 4. The stacking pattern in the direction **a**, which is the vertical direction in Fig. 10, can be described as RLRLRLRL in the monoclinic polymorph and as

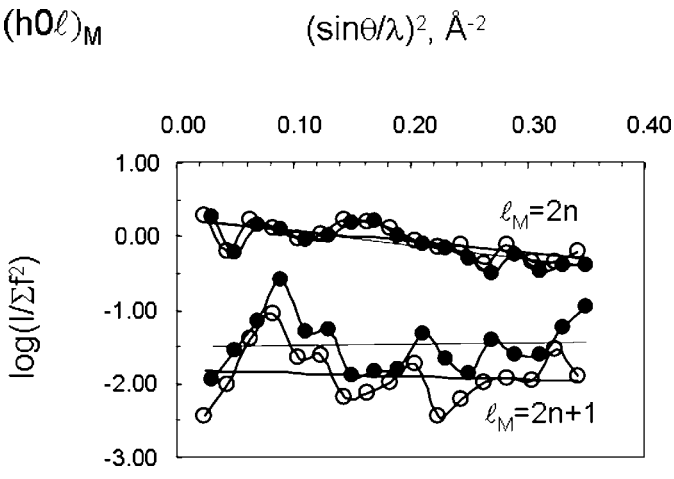

Figure 9
Separate Wilson plots for the $(h0\ell)_M$, $\ell = 2n$ and $(h0\ell)_M$, $\ell = 2n + 1$ reflections measured at 90 K for a crystal grown from acetone (filled circles; data measured with Mo $K\alpha$ radiation from a sealed tube) and for a crystal grown from toluene (open circles; data measured with Cu $K\alpha$ radiation from a rotating-anode source). The $(h0\ell)_M$, $\ell = 2n + 1$ reflections for the crystal grown from acetone are relatively more intense because the crystal grown from acetone is more ordered. The origin of the vertical scale is arbitrary; the overlap of the two sets of $\ell = 2n$ points has been maximized.

RRLLRRLL in the orthorhombic polymorph (where R, for right, and L, for left, refer to the directions of the P—O vector in the top half of Fig. 10). The length a_{ortho} (*i.e.* the vertical direction in Fig. 10) is just under twice $a_{mono}\sin\beta_{mono}$; the ratio at room temperature is 1.952 (Thomas & Hamor, 1993; Spek, 1987). At room temperature this second monoclinic polymorph is 1.5% less dense than the orthorhombic polymorph and so is presumed to be less stable near 300 K. The second monoclinic polymorph was also discovered much later than the orthorhombic and first monoclinic polymorphs (Spek, 1987).

The ratios of the average cell constants for the CHDTPPO and TPPO structures are given in Table 4. In order to accommodate the *rac*-1,2-CHD ribbon the TPPO layer must shrink by *ca* 2% along $\mathbf{b}_{CHDTTPO,T}$ (the horizontal direction in the upper half of Fig. 10; triclinic axes) and expand by *ca* 2–3% along $\mathbf{a}_{CHDTPPO,T}$ (the horizontal direction in the lower half of Fig. 10). The γ angle must increase by *ca* 0.5° from 90°. The $\mathbf{b}_T$ direction in which the TPPO layers are compressed is the direction of the hydrogen-bonded *rac*-1,2-CHD ribbons; the $\mathbf{a}_T$ directions in which the TPPO layers expand is the direction in which adjacent *rac*-1,2-CHD ribbons are in contact.

The first monoclinic TPPO polymorph (Brock *et al.*, 1985) and the third (Lenstra, 2007) have somewhat different molecular conformations and quite different packing.

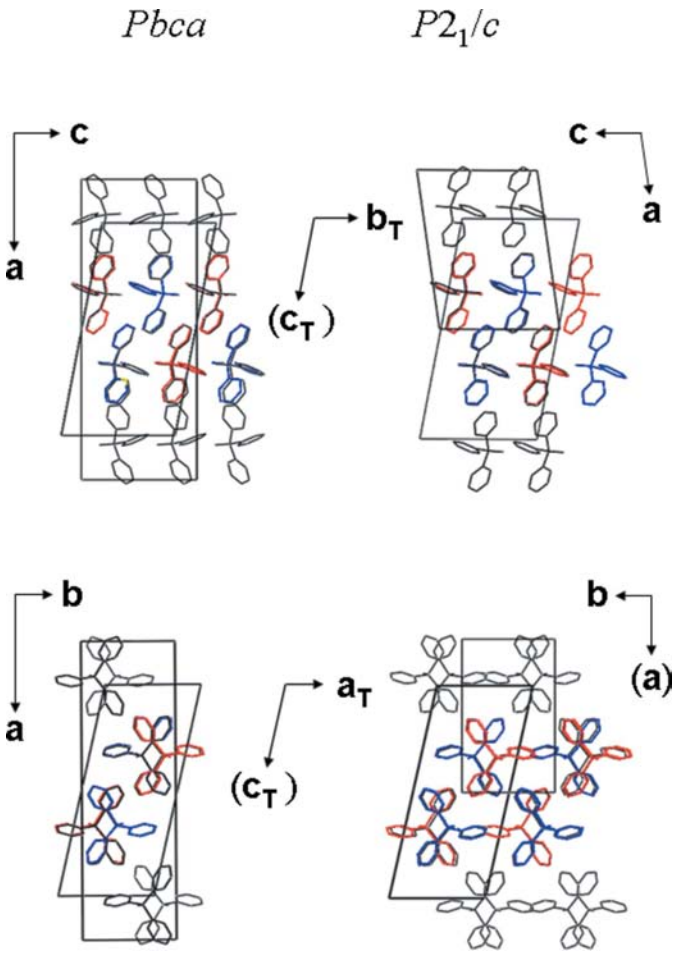

Figure 10
Overlays (left) of the TPPO layer of the CHDTPPO structure at 90 K (as determined for a crystal grown from acetone) with the structure of the *Pbca* polymorph determined at 100 K (Brock *et al.*, 1985) and (right) of the CHDTPPO structure at 294 K (also for a crystal grown from acetone) with the structure of the second monoclinic polymorph at room temperature (Spek, 1987). The upper drawings are related to the lower drawings by a rotation of 90° around the vertical axis. Labels for axes that are more than 1° out of the plane of the drawing are shown in parentheses.

3.3. *rac*-1,2-CHD ribbons

The first question is whether or not there is disorder in individual hydrogen-bonded ribbons. The second is how similar this ribbon is to those seen in other structures.

3.3.1. Disorder in the *rac*-1,2-CHD ribbons. If there is no disorder in a *rac*-1,2-CHD ribbon then each of the two symmetry-independent *rac*-1,2-CHD molecules in CHDTPPO must make a dimer with an inversion-related molecule (see Fig. 2). The two independent molecules alternate along the ribbon edges (or ladder rails); molecules adjacent in a rail are heterochiral. We believe that the successful location and restrained refinements of the hydroxyl H atoms of the major component for most datasets suggests that individual ribbons are at least mostly ordered. The problems with locating and refining those H atoms for the minor component in the triclinic refinement and for both components in the monoclinic approximation support this conclusion, as do the values of the *rac*-1,2-CHD occupancy factors that are far from 0.5 (see Table 2). The real twofold axes that would relate adjacent *rac*-1,2-CHD dimers in a true *C*2/*c* structure would require that the ladder rails be homochiral. These axes also lead to C—O—H angles and/or O—H···O distances and angles that are strained at best and perhaps impossible. An approximate twofold axis relating adjacent major and minor *rac*-1,2-CHD components would cause the same problem.

In *rac*-1,2-cyclohexyl-1,2-diol (GEJMEO; Patrick & Brock, 2006; *C*2/*c*) hydrogen-bonded dimers at inversion centers are related by twofold rotation axes to give the same hydrogen-bond pattern that would be found for the dimer ribbon in CHDTPPO if its space group were *C*2/*c*. In GEJMEO the molecules in each rail are homochiral; the hydroxyl H atoms are all disordered over two positions. The C—O—H and O—H···O distances and angles are normal, but probably only because adjacent $R_4^4(8)$ rings are offset by 0.44 Å in the **b** direction [*i.e.* parallel to the twofold axes and perpendicular to the ribbon axis; see part (*c*) of Fig. 2]. Such an offset would be impossible in the CHDTPPO structure because the ribbon must fit tightly into the groove in the underlying TPPO layer. In the CHDTPPO structure all the $R_4^4(8)$ rings must be related by a translation or pseudotranslation along the ribbon axis rather than lying alternately above and below that axis. The differences between the dimer ribbons in GEJMEO and CHDTPPO also suggest that individual *rac*-1,2-CHD ribbons in CHDTPPO are completely, or at least almost completely, ordered.

We also believe that the *rac*-1,2-CHD dimer ribbons in a layer at $z_T = 0$ or at $x_M = 0$ or $\frac{1}{2}$ (see Fig. 1) are nearly always related by inversion symmetry. The argument for the symmetry correlation within a dimer ribbon is given above. Correlation between ribbons adjacent in a layer occurs because if the inversion symmetry between ribbons is not obeyed then there are short contacts between axial H atoms. At room temperature the contacts H5*A*2(x, y, z)$\cdots$H2*A*′($2-x, -y, -z$) and H2*B*(x, y, z)$\cdots$H5*B*3($-x, 1-y, -z$) would be quite short at 2.31–2.34 and 2.26–2.31 Å (ranges are given for the crystals grown from the different solvents). For each molecule pair there are two such contacts because of the inversion symmetry. We believe those contacts to be unfavorable enough to require that the inversion symmetry be obeyed. These contacts are even shorter at 90 K (2.22–2.25 and 2.23–2.30 Å), but since the crystals were grown at room temperature and since the *rac*-1,2-CHD enantiomers cannot interconvert, it is the distances at room temperature that are more important.

Another argument for order within the *rac*-1,2-CHD layers but disorder between layers is the streaking along $\mathbf{c}_T^* = \mathbf{a}_M^*$ seen in several diffraction patterns (see Figs. 5 and 6).

3.3.2. Comparison with other *rac*-1,2-CHD dimer ribbons. *rac*-1,2-CHD itself does not form any structure that contains a hydrogen-bonded dimer ribbon (Lloyd *et al.*, 2007, and references therein). We found only two structures in the CSD of *trans vic*-diols $C_nH_m(OH)_2$ that form dimer ribbons and have heterochiral rails: WOVDOA (Clausen *et al.*, 2001) and ZIVCEM (Schaefer *et al.*, 1996). Both structures have $Z' = 2$, with each independent molecule forming a dimer around an inversion center. The cell translations at room temperature along the hydrogen-bonded ribbons are 5.28 Å (WOVDOA) and 5.40 Å (ZIVCEM) per dimer.[5] The corresponding distance in CHDTPPO (*i.e.* b_T) is 5.50 Å. These values are consistent with the idea that in the CHDTPPO structure the *rac*-1,2-CHD ribbon is slightly stretched along the $\mathbf{b}_T$, axis while the TPPO layer is slightly compressed.

3.4. Schematic phase diagram

A schematic *T*–*X* phase diagram (Fig. 11) was calculated from the measured temperatures and heats of fusion under the assumption that the solutions behave ideally (see Jacques *et al.*, 1981). The temperatures and heats of fusion for *rac*-1,2-CHD and TPPO were taken as the lowest values in the measured ranges, while the values for the CHDTPPO compound are the highest in the ranges; these choices maximize the region in which the CHDTPPO phase is expected to be stable. If T_{fus} and $\Delta_{fus}H^\circ$ are chosen to be in the middle of the measured ranges, there is no region in which CHDTPPO crystals are predicted to be thermodynamically stable.

CHDTPPO crystals were not, however, grown from the melt, but from solutions. The phase diagram should therefore have a third dimension corresponding to the solvent. On the other hand, it is generally assumed (see Jacques *et al.*, 1981) that the appearance of sections of a two-solute phase diagram does not vary much with solvent mole fraction. If that assumption is valid and if the assumptions inherent in the calculation of the phase diagram are correct, then many crystals of pure TPPO should precipitate before any crystals of CHDTPPO form. This prediction is at variance with our observations, which suggest that CHDTPPO crystals dominate the precipitate.

4. Discussion

4.1. TPPO polymorphs

The growth characteristics of the TPPO polymorphs, as well as their structural relationships, are important to the understanding of why the CHDTPPO compound forms, particularly since the predicted phase diagram indicates numerous TPPO crystals should precipitate from a solution equimolar in TPPO and *rac*-1,2-CHD before any crystals of the CHDTPPO compound grow.

In 1983 considerable time was spent growing crystals of TPPO in an attempt to isolate the orthorhombic *Pbca* polymorph (see Brock *et al.*, 1985). Most TPPO crystals grown at room temperature from a variety of solvents were the first monoclinic polymorph, which is the densest of the four by 0.6% at room temperature but which has the weakest (as judged by length) CH$\cdots$O=P interactions (see Table 3). Orthorhombic TPPO crystals were first obtained from *n*-

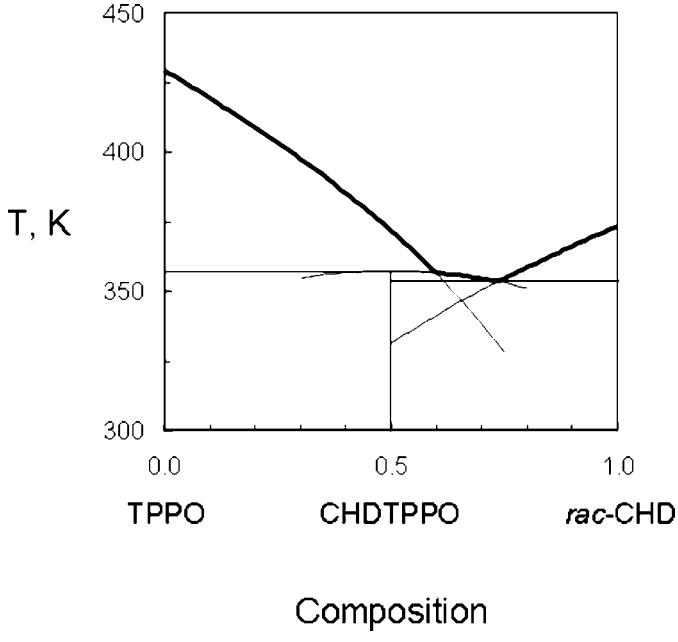

Figure 11
Idealized solid–liquid phase diagram calculated for TPPO and *rac*-1,2-CHD from the measured temperatures and heats of fusion (see Jacques *et al.*, 1981). The exact T_{fus} and $\Delta_{fus}H^\circ$ values were chosen from the ranges measured in order to maximize the region of stability of the CHDTPPO compound (see text).

[5] The hydroxyl H atoms in WOVDOA and ZIVCEM indicate a hydrogen-bond pattern similar to that found for the major *rac*-1,2-CHD component in CHDTPPO. Distances and angles involving these H atoms are unexceptional except for one of the four hydroxyl H atoms in WOVDOA, which is clearly in the wrong place.

hexane, from which both the *Pbca* and first monoclinic polymorphs precipitate. The *Pbca* crystals, which were easy to distinguish visually from the monoclinic crystals, were then used to seed toluene solutions, which otherwise produced only monoclinic crystals.

The successful seeding of solutions with the *Pbca* polymorph suggests it and the first monoclinic polymorph have similar stabilities near room temperature; it is likely that the *Pbca* polymorph is more thermodynamically stable near 295 K. Since crystals of the second and third monoclinic polymorphs occur together (Lenstra, 2007), these two phases probably also have similar stabilities. The lower density of the second monoclinic polymorph suggests it and the third monoclinic polymorph might grow at higher temperatures and then persist as metastable phases when cooled to room temperature.

The *Pbca* TPPO crystals grown in 1983 were thin along **a**, which is the direction perpendicular to the TPPO layers discussed above (*i.e.* the vertical direction in Fig. 10). The *Pbca* crystals are elongated along **c**, which is analogous to the axis $\mathbf{b}_T = \mathbf{c}_M$ of CHDTPPO, *i.e.* the axis of the hydrogen-bonded *rac*-1,2-CHD ribbons. This direction is also the direction in which the CH$\cdots$O=P interactions of the *Pbca* polymorph are strongest. The *Pbca* TPPO crystals and the CHDTPPO crystals have similar habits, except that the *Pbca* laths are thinner and the end faces indicate orthorhombic symmetry. Crystals of the first monoclinic polymorph were larger, more equidimensional and more multifaceted.

These observations suggest that growth in the direction perpendicular to the TPPO layers is slow both in the *Pbca* polymorph of TPPO and in the compound CHDTPPO. Growth along directions within a layer is faster because of the favorable CH$\cdots$O=P interactions in both crystals and because of the OH$\cdots$O bonds in CHDTPPO.

The *Pbca* polymorph may be difficult to obtain not because it is less stable than other polymorphs, but because nucleation and growth is slower. The existence of the same TPPO bilayers in three different structures (*i.e.* in two TPPO polymorphs and in the CHDTPPO compound) suggests that the packing in those bilayers is quite favorable. Growth perpendicular to those layers, however, seems to be slow.

4.2. Why does the compound form?

The CHDTPPO compound may well be a kinetic product. Crystals of the CHDTPPO co-crystal may be a little more efficiently packed than crystals of TPPO (see Table 3), but the CH$\cdots$O=P distances are longer. If the calculated phase diagram is at least basically correct then evaporation of solutions equimolar in *rac*-1,2-CHD and TPPO should precipitate crystals of TPPO first. The compound CHDTPPO should be found as a minor product and as part of a fine-grained eutectic. It therefore seems likely that the CHDTPPO compound forms because its crystals nucleate and grow better than crystals of pure TPPO. Fragments of dimer ribbons of *rac*-1,2-CHD molecules almost certainly exist in solution as do aggregates of TPPO molecules, some of which are almost certainly like the molecular bilayers seen in the compound. Because the growth of pure TPPO perpendicular to the layers is slow, because the CHD ribbons just happen to fit well in the layer grooves (see Table 4), and because the hydrogen bonding along the dimer ribbon promotes crystal growth, the crystals of the compound grow better than the crystals of orthorhombic TPPO or of the first monoclinic TPPO polymorph.

4.3. Communication through the TPPO layers

There are very few short contacts between molecules in the TPPO layers and molecules in the *rac*-1,2-CHD layers and none of them appears to be especially favorable. The most important repulsive contacts are between C13*B* (and perhaps H13*B*) of the second TPPO molecule and the axial H atom of C1*B*, which is attached to a hydroxyl group of the second 1,2-CHD molecule; the distance is 2.63 Å[6] for the crystal grown from acetone and measured at 90 K. The corresponding contact for C13*A* and the H atom of C1*A* is not short because the configuration at C1*A* is *S* rather than *R* so that the axial H atom is pointing in the opposite direction, but the contact of C13*A* to the axial H atom of the low-occupancy C1*A*′ atom would be even shorter (2.48 Å). [The corresponding distance in the monoclinic refinement is intermediate (2.56 Å)]. It seems that an important difference between the two independent TPPO molecules is a very slight shift of the ring containing C13*B* to partially relieve the unfavorable contact. If the *rac*-1,2-CHD molecules in a layer are, as we expect, almost completely ordered, then the contact involving the minor component C1*A*′ does not need to be considered. There are also *very* small differences (*e.g.* a rotation of several degrees) between phenyl rings containing C23*A* and C23*B*, and containing C33*A* and C33*B*.

The observed disorder then occurs because communication through the TPPO layers of this slight shift in the ring containing C13*B* is imperfect. Other than the CH$\cdots$O=P contacts (see Table 3) there are no really short contacts within the TPPO layer. The distinction between the two independent molecules could be lost so easily that it is the partial ordering, rather than the disorder, that is a surprise.

4.4. Correlation of layers *versus* anticorrelation

If all CHD layers were ordered and if there were neither correlation nor anticorrelation between adjacent CHD layers then the crystal would be best described by the space group *C*2/*c*. If CHD molecules related by the translation $[0\,0\,1]_T = [\frac{1}{2}\,-\frac{1}{2}\,0]_M$ were always enantiomers (*i.e.* if the sites were anticorrelated) then the space-group symmetry would be reduced to $P2_1/n$. All twofold axes would be lost, as would the inversion centers at $x_M = \frac{1}{4}$ and $\frac{3}{4}$, and the *c* glide planes. The twofold screw axes and the *n* glides, however, would be retained. If, on the other hand, CHD molecules related by the translation $[0\,0\,1]_T = [\frac{1}{2}\,-\frac{1}{2}\,0]_M$ were always homochiral, then

[6] The distances to H atoms are necessarily approximate since the H atoms are in calculated positions. The calculated C$\cdots$H distance is so short that the axial H atom is almost certainly slightly displaced from the expected position.

all twofold axes and all glide planes would be lost and the space group would become $P\overline{1}$. In the case of either correlation or anticorrelation the number of independent formula units (Z') would change from one to two.

If the layers are fully ordered then all CHD molecules on the same 'side' of a layer (*e.g.* all CHD molecules with centroids having x_M or z_T in the range 0.0–0.1) are homochiral. In a $P2_1/n$ domain adjacent layers would be related by a 2_1 axis; while in a $P\overline{1}$ domain the layers would be related by translation.

There is clear evidence that CHD molecules related by the translation $[0\ 0\ 1]_T = [\frac{1}{2}\ -\frac{1}{2}\ 0]_M$ are more often homochiral than heterochiral, with the correlation being strongest in the crystals grown from acetone. The small but significant deviations of two cell angles from 90°, the unsatisfactory averaging in Laue group $2/m$ of reflection intensities, and the deviations of the occupancy factors from 0.5 all point to space group $P\overline{1}$ and thus to some degree of correlation. Neither anticorrelation nor complete disorder can explain these observations.

It is difficult, however, to rule out the possibility of the presence of some domains in which there is anticorrelation (space group $P2_1/n$). There is no class of reflections that would have measurable intensity in $P2_1/n$ that would not also have intensity in $P\overline{1}$. [Note that violations of the $(h0\ell)_M$, $h + \ell = 2n$ condition of $P2_1/n$ can be seen easily in Figs. 4 and 5]. The occupancy factors for the enantiomers in the $P\overline{1}$ model are intermediate between 0.0 (as they would be for a perfectly ordered triclinic structure) and 0.5 (as they would be for a $P2_1/n$ structure refined in $P\overline{1}$). These occupancy factors could indicate the presence of both triclinic and monoclinic domains or could just correspond to disorder in the triclinic domains.

Diffraction experiments of the type we have done cannot distinguish between these last two possibilities. We think, however, that very imperfect correlation ($P\overline{1}$ and $C2/c$ domains) is a more likely explanation than a combination of imperfect correlation and imperfect anticorrelation ($P\overline{1}$, $P2_1/n$ and $C2/c$ domains). As correlation of layers is observed it must lower the energy enough to offset the entropy loss resulting from the ordering. It seems to us unlikely that correlation and anticorrelation could both lower the energy to a similar extent, but that possibility cannot be ruled out.

4.5. Is there a phase transition?

It seems unlikely that an individual CHDTPPO crystal could undergo a phase transformation at elevated temperature from the lower symmetry triclinic form to a higher symmetry monoclinic form because such a transformation would require either interconversion of 1,2-CHD enantiomers or large translations of the ribbons. For similar reasons slow cooling is not expected to produce increased order.

It might then seem that crystal growth at elevated temperatures would result in monoclinic crystals best described in $C2/c$. We suspect, however, that for crystals grown at somewhat elevated temperatures individual ribbons would remain mostly ordered because the disorder associated with monoclinic symmetry does not seem to permit a favorable *rac*-1,2-CHD hydrogen-bonding arrangement. In any event all the crystals studied were grown at essentially the same temperature.

4.6. Variation of order with solvent

It seems likely then that the degree of order is determined during crystal growth. The reason for the variation of ordering with crystallization solvent is unknown. It might be expected that crystals grown more slowly would be more ordered, but if anything the reverse seems to be the case because crystal growth from acetone was much more rapid than from toluene. It is possible that the hydrogen-bonding capabilities of the three solvents play a role, but we can propose no mechanism. Interactions of the phenyl rings of the toluene and TPPO molecules may also be a factor.

5. Summary

The 1:1 co-crystal of *rac*-1,2-CHD and TPPO is unusual because of its existence and its variation in degree of order with solvent. Also unusual is the transmission through a very pseudosymmetric TPPO layer of the information about the enantiomeric ordering in a *rac*-1,2-CHD layer. The chances of another pair of unrelated molecules fitting together to fill space as well as these two do are very small indeed. The transmission through a very pseudosymmetric TPPO layer of information about the *R*,*R*/*S*,*S* ordering in a *rac*-1,2-CHD layer is a testament to the exquisite sensitivity of crystals to the exact locations of atoms. That the degree of transmission might depend on the solvent from which the crystals are grown is a surprise. This compound would be a good candidate for a study of crystal growth because it is easy to make from compounds that are inexpensive to purchase and easy to handle.

We are grateful to the Kentucky EPSCoR program (NSF Grant EHR-91-08764) for financial support and to the National Science Foundation (MRI No. 0319176) for funds to purchase the Bruker–Nonius X8 Proteum diffractometer. We thank Professor A. Spek (Utrecht) for bringing the fourth polymorph of TPPO to our attention. We thank a referee for posing stimulating questions.

References

Allen, F. H. (2002). *Acta Cryst.* B**58**, 380–388.
Andrews, L. C., Bernstein, H. J. & Pelletier, G. A. (1980). *Acta Cryst.* A**36**, 248–252.
Beurskens, P. T.*et al.* (1983). *DIRDIF*. Technical Report 1983/1. Crystallography Laboratory, Toemooiveld, 6525 ED Nijmegen, The Netherlands.
Brock, C. P. (2002). *Acta Cryst.* B**58**, 1025–1031.
Brock, C. P., Schweizer, W. B. & Dunitz, J. D. (1985). *J. Am. Chem. Soc.* **107**, 6964–6970.
Bruker–Nonius (2004). *APEX*2. Bruker–Nonius AXS, Madison, Wisconsin.
Clausen, C., Wartchow, R. & Butenschon, H. (2001). *Eur. J. Org. Chem.* pp. 93–113.
Desiraju, G. R. (1996). *Acc. Chem. Res.* **29**, 441–449.

Desiraju, G. R. & Steiner, T. (1999). *The Weak Hydrogen Bond in Structural Chemistry and Biology*. Oxford University Press.
Etter, M. C. & Baures, P. W. (1988). *J. Am. Chem. Soc.* **110**, 639–640.
Falvello, L. R., Tomas, M. & Soler, T. (2002). Private communication (refcode TPEPHO10). Cambridge Crystallographic Data Centre, Cambridge, England.
Herbstein, F. H. (2005). *Crystalline Molecular Complexes and Compounds*, 1st ed. Oxford University Press.
Jacques, J., Collet, A. & Wilen, S. H. (1981). *Enantiomers, Racemates, and Resolutions*. New York: John Wiley and Sons.
Jeffrey, G. A. (1997). *An Introduction to Hydrogen Bonding*. New York: Oxford University Press.
Lenstra, A. T. (2007). Private communication (refcode TPEPHO12). Cambridge Crystallographic Data Centre, Cambridge, England.
Lloyd, M. A., Patterson, G. E., Simpson, G. H., Duncan, L. L., King, D. P., Fu, Y., Patrick, B. O., Parkin, S. & Brock, C. P. (2007). *Acta Cryst.* B**63**, 433–447.
Macrae, C. F., Edgington, P. R., McCabe, P., Pidcock, E., Shields, G. P., Taylor, R., Towler, M. & van de Streek, J. (2006). *J. Appl. Cryst.* **39**, 453–457.
Main, P., Lessinger, L., Woolfson, M. M., Germain, G. & Declercq, J.-P. (1977). *MULTAN*77. Universities of York and Louvain.
Niggli, P. (1928). *Handbuch der Experimentalphysik*, Vol. 7, Part 1. Leipzig: Akademische Verlagsgesellschaft.
Nonius (1999). *COLLECT*. Nonius BV, Delft, The Netherlands.
Otwinowski, Z. & Minor, W. (1997). *Methods Enzymol.* **276**, 307–326.
Patrick, B. O. & Brock, C. P. (2006). *Acta Cryst.* B**62**, 488–497.
Schaefer, W. P., Henling, L. M., McBay, H. C. & Abulū, J. (1996). *Acta Cryst.* C**52**, 104–107.
Shape Software (2003). *SHAPE*, Version 7.0. Kingsport, Tennessee.
Sheldrick, G. M. (1997). *SHELXL*97. University of Göttingen, Germany.
Spek, A. L. (1987). *Acta Cryst.* C**43**, 1233–1235.
Spek, A. L. (2003). *J. Appl. Cryst.* **36**, 7–13.
Thomas, J. A. & Hamor, T. A. (1993). *Acta Cryst.* C**49**, 355–357.
Xia, A., Selegue, J. P., Carrillo, A., Patrick, B. O., Parkin, S. & Brock, C. P. (2001). *Acta Cryst.* B**57**, 507–516.
Xia, A., Selegue, J. P., Carrillo, A., Patrick, B. O., Parkin, S. & Brock, C. P. (2002). *Acta Cryst.* B**58**, 565.